Cell PRESS
Structure
Article

Crystal Structures of Phd-Doc, HigA, and YeeU Establish Multiple Evolutionary Links between Microbial Growth-Regulating Toxin-Antitoxin Systems

Mark A. Arbing,[1,6] Samuel K. Handelman,[1,2] Alexandre P. Kuzin,[1,2] Grégory Verdon,[1,7] Chi Wang,[1] Min Su,[1,2] Francesca P. Rothenbacher,[4] Mariam Abashidze,[1,2] Mohan Liu,[4,8] Jennifer M. Hurley,[4,9] Rong Xiao,[2,5] Thomas Acton,[2,5] Masayori Inouye,[2,3,5] Gaetano T. Montelione,[2,5] Nancy A. Woychik,[2,4] and John F. Hunt[1,2,*]

[1]Department of Biological Sciences, Columbia University, 702 Fairchild Center, MC2434, New York, NY 10027, USA
[2]Northeast Structural Genomics Consortium
[3]Department of Biochemistry, Robert Wood Johnson Medical School, University of Medicine and Dentistry of New Jersey, Piscataway, NJ 08854, USA
[4]Department of Molecular Genetics, Microbiology, and Immunology, Robert Wood Johnson Medical School, University of Medicine and Dentistry of New Jersey, Piscataway, NJ 08854, USA
[5]Center for Advanced Technology and Medicine and Department of Molecular Biology and Biochemistry, Rutgers University, Piscataway, NJ 08854, USA
[6]Present address: UCLA-DOE Institute for Genomics and Proteomics, University of California, Los Angeles, Los Angeles, CA 90095, USA
[7]Present address: Department of Physiology and Biophysics, Weill Medical College of Cornell University, New York, NY 10065, USA
[8]Present address: Department of Molecular Pharmacology and Experimental Therapeutics, Mayo Clinic, Rochester, MN 55902, USA
[9]Present address: Department of Genetics, Dartmouth Medical School, Hanover, NH 03755, USA
*Correspondence: jfhunt@biology.columbia.edu
DOI 10.1016/j.str.2010.04.018

SUMMARY

Bacterial toxin-antitoxin (TA) systems serve a variety of physiological functions including regulation of cell growth and maintenance of foreign genetic elements. Sequence analyses suggest that TA families are linked by complex evolutionary relationships reflecting likely swapping of functional domains between different TA families. Our crystal structures of Phd-Doc from bacteriophage P1, the HigA antitoxin from *Escherichia coli* CFT073, and YeeU of the YeeUWV systems from *E. coli* K12 and *Shigella flexneri* confirm this inference and reveal additional, unanticipated structural relationships. The growth-regulating Doc toxin exhibits structural similarity to secreted virulence factors that are toxic for eukaryotic target cells. The Phd antitoxin possesses the same fold as both the YefM and NE2111 antitoxins that inhibit structurally unrelated toxins. YeeU, which has an antitoxin-like activity that represses toxin expression, is structurally similar to the ribosome-interacting toxins YoeB and RelE. These observations suggest extensive functional exchanges have occurred between TA systems during bacterial evolution.

INTRODUCTION

Microbial toxin-antitoxin (TA) systems are employed by bacterial, bacteriophage, and autonomous extrachromosomal DNA elements to regulate bacterial growth. Plasmid- and phage-encoded TA systems serve as "addiction modules" that maintain their genetic material within host cells by exerting bacteriostatic/bacteriocidal effects. Chromosomal TA systems are thought to reversibly attenuate bacterial growth under conditions of nutritional or environmental stress (Condon, 2006). The vast majority of TA systems are believed to employ a common mechanism of action in which proteolytic degradation of the antitoxin allows the toxin to kill the cell or send it into a quiescent state. For chromosomal systems, removal of the environmental stressor allows newly synthesized antitoxin to complex with the existing toxin, thus reversing toxicity and allowing resumption of normal growth. This process may become bacteriocidal under conditions in which the quiescent state can no longer be maintained or the ability to synthesize new antitoxin is lost (Pedersen et al., 2002). For plasmid-encoded systems, toxicity occurs when a daughter cell is cured of the foreign genetic element and loses the ability to synthesize new antitoxin molecules. As the existing antitoxins are degraded, toxin activity results in irreversible postsegregational killing of the cured cell. Consequently, the killing of cured cells maintains phage or plasmid DNA in bacterial populations.

Valuable insight into the structure and function of TA systems has been gained from the crystal structures of individual toxin and antitoxin molecules (Hargreaves et al., 2002; Kamada and Hanaoka, 2005; Loris et al., 1999, 2003), complete TA complexes (Kamada and Hanaoka, 2005; Kamada et al., 2003; Mattison et al., 2006; Miallau et al., 2009; Takagi et al., 2005), and complexes of toxins with their cellular targets (Dao-Thi et al., 2004; Kamphuis et al., 2006). These structures have revealed information on toxin-antitoxin complex assembly, how antitoxins inhibit their toxin partners, and details on the mechanisms of toxin activity. In particular, the structures of the YoeB-YefM (Kamada and Hanaoka, 2005) and RelBE systems (Takagi et al., 2005) have revealed that the YoeB and RelE toxins, despite sharing only 13% sequence identity, are structurally similar to one another and have a similar fold to a family of microbial RNases (Kamada and Hanaoka, 2005). Amino acid residues

implicated in the function of the toxins and related RNases are clustered on one face of the central β sheet that forms the core of these enzymes, although the specific locations of the catalytic residues are not conserved.

There is considerable functional diversity even among structurally related toxins. Many inhibit protein synthesis and can be broadly classified as either ribosome-dependent or ribosome-independent mRNA interferases (Yamaguchi and Inouye, 2009; Zhang et al., 2009). The structurally unrelated Doc and YoeB toxins are ribosome-dependent mRNA interferases that inhibit protein translation using different mechanisms. Doc, an α-helical bundle protein, interacts with the 30S ribosomal subunit and blocks translation (Liu et al., 2008) whereas YoeB, which has a microbial RNase fold, interacts with the 50S ribosomal subunit and prevents translation initiation (Zhang and Inouye, 2009). RelE, which is structurally similar to YoeB, is also a ribosome-dependent mRNA interferase that cleaves mRNA positioned in the ribosomal A site (Pedersen et al., 2003). HigB, which is homologous to RelE and YoeB (Pandey and Gerdes, 2005), is a sequence-specific endoribonuclease whose activity is dependent on association with the 50S ribosomal subunit (Christensen-Dalsgaard and Gerdes, 2006; Hurley and Woychik, 2009). MazF, a ribosome-independent mRNA interferase, cleaves single-stranded RNA, specifically recognizing the sequence ACA (Zhang et al., 2003). The MazF structure (Kamada et al., 2003) revealed that it is homologous to two other toxins: Kid/PemK of the R100 plasmid and CcdB of the F plasmid. Whereas the MazF and Kid toxins have similar biochemical functions as sequence-specific, ribosome-independent mRNA interferases (Zhang et al., 2004), CcdB instead inhibits DNA replication by binding to DNA gyrase (Miki et al., 1992).

In contrast to toxins, antitoxin function is relatively invariant despite dramatic differences in the sequences and folds of antitoxins from different families. Antitoxins are composed of two domains which have distinct functions. The "neutralization" domain binds to the toxin and neutralizes it, either by occluding its active site (Kamada and Hanaoka, 2005; Kamada et al., 2003; Miallau et al., 2009) or by changing its shape such that it can no longer interact with its cellular target (Garcia-Pino et al., 2008; Takagi et al., 2005). The other domain is a DNA-binding domain that represses transcription by binding near the promoter of the operon encoding the TA complex. This repression is typically mediated by the complete TA complex, although it can be mediated by the antitoxin alone (Kedzierska et al., 2007). To date, there is only one TA system in which an antitoxin-like activity has deviated from this general scheme of toxin neutralization and transcriptional autoregulation. YeeU of the YeeUV(W) TA system appears to inhibit the toxicity of the YeeV toxin without directly binding to it. YeeU is believed to function as either a transcriptional or translational attenuator of YeeV expression, by binding to a short (~70 bp) nucleotide sequence between the *yeeU* and *yeeV* genes (Brown and Shaw, 2003). YeeU represents the first example where a proteinaceous antitoxin controls toxin activity solely via regulation of toxin expression without directly binding to the toxin to neutralize it. The function of YeeW, the product of the third gene in the *yeeUVW* operon, is unknown.

Many bacteria harbor an abundance of chromosomal TA systems. The *Escherichia coli* genome encodes at least seven systems from six different sequence families, whereas the *Mycobacterium tuberculosis* genome encodes a minimum of 57 TA systems, many from the VapBC family (Makarova et al., 2009). Sequence-profiling analyses suggested that there are four major families of TA systems that evolved independently (Anantharaman and Aravind, 2003; Pandey and Gerdes, 2005), along with an abundance of subfamilies that resulted from the swapping of individual components (either toxin or antitoxin genes) or domains of these components between the major families (Smith and Magnuson, 2004). A more recent study using a combination of sequence analysis methods found many new families of TA systems that had not been described previously (Makarova et al., 2009). Some of these new families were specific to certain lineages of archaea or eubacteria. In some instances, toxins or antitoxins from known families were found to exist in the absence of their cognate partner, such as, for example, the *Myxococcus xanthus* MazF gene, which is not cotranscribed with its cognate antitoxin (Nariya and Inouye, 2008). Although the functions of these "solo" components have yet to be investigated experimentally, Makarova et al. hypothesized that they would most likely have biochemical activities similar to the homologs found within canonical two-component TA systems. Specifically, they proposed that the transcriptional regulation activity of solo antitoxins would regulate expression of particular genes, whereas solo toxins would continue to target particular biochemical processes potentially modulating cellular growth. The evolutionary relationships between TA systems, as predicted by phylogenetic analyses, have been confirmed in part by crystallographic studies showing structural similarities between YoeB and RelE (Kamada and Hanaoka, 2005) and between the Kis, CcdB, and MazF toxins (Kamada et al., 2003). However, additional structural information is needed to elucidate these complex relationships.

We herein prove additional structural relationships between TA systems. We have determined crystal structures of the P1 bacteriophage toxin Doc (*d*eath *o*n *c*uring) in complex with its antitoxin Phd (*p*revents *h*ost *d*eath), of the HigA antitoxin of the HigBA TA system, and of the YeeU protein of the YeeUV(W) TA system. These structures all establish homology to components from different TA systems. The structure of Phd is observed to be homologous to an antitoxin that neutralizes a toxin with a related endonuclease activity but a structure unrelated to Doc, thereby proving that shuffling of antitoxins between different TA systems occurred over the course of evolution. The structure of the HigA antitoxin demonstrates a complementary form of shuffling by showing that different antitoxin folds are used to neutralize homologous YefM/YoeB-family toxins. The structure of the YeeU antitoxin demonstrates a third kind of evolutionary relationship between TA systems. Although YeeU has a fold related to the YoeB/RelE nucleic acid-hydrolyzing toxins, YeeU is a nucleic acid-binding factor with antitoxin-like activity, suggesting evolutionary exchange between toxin and antitoxin families. Our results thus clarify the complex evolutionary relationships underlying the proliferation of TA systems.

RESULTS AND DISCUSSION

Phylogenetic Relationships between TA Systems

Figure 1 presents a series of cladograms summarizing the likely evolutionary relationships between TA system components

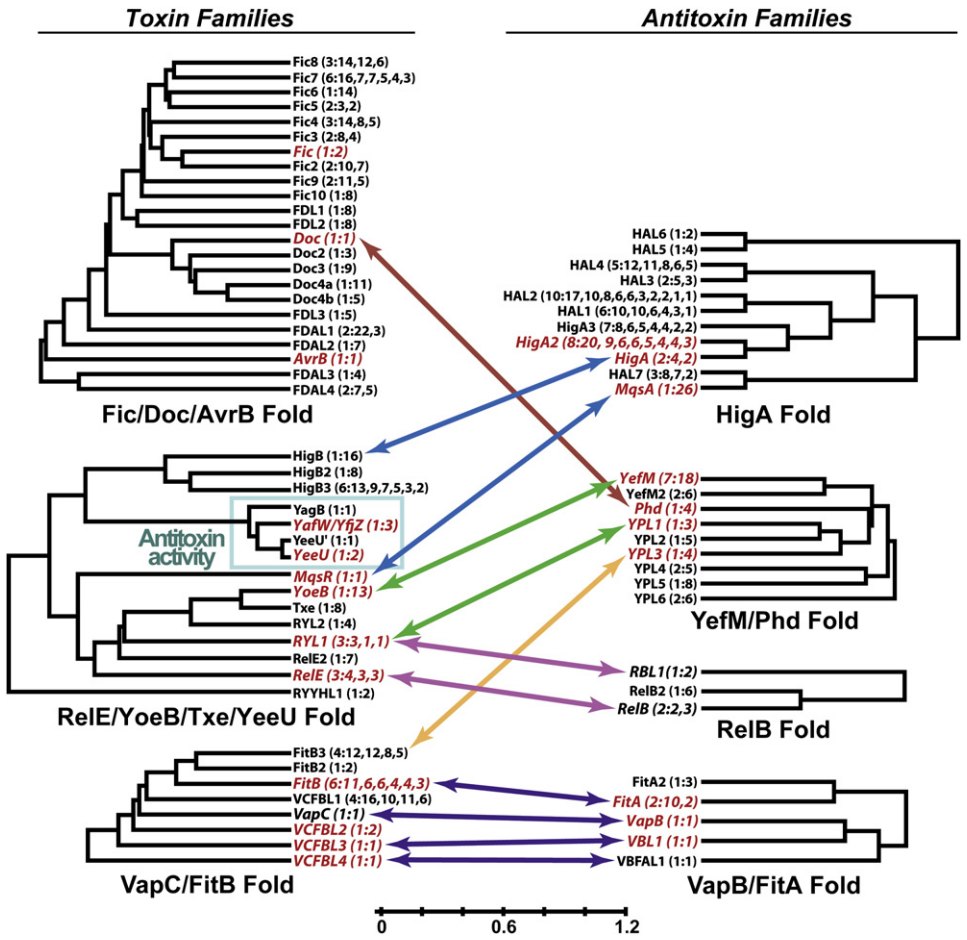

Figure 1. Evolutionary Relationships between Components of Bacterial Toxin-Antitoxin Systems

Cladograms modeling the evolutionary relationship between a representative member of toxin (left) and antitoxin (right) families were prepared using MEGA (as described in Experimental Procedures). Structurally related proteins are grouped together into single cladograms. The double-headed arrows connect cognate toxins and antitoxins from representative TA systems. Branches of families that have a member whose structure has been experimentally determined are labeled in red.

related to the crystal structures presented in this paper. These relationships were inferred from structural similarity combined with sequence profiling of predicted protein families from 474 fully sequenced microbial genomes. Homologous proteins were split into putative functional families based on simultaneous occurrence of two homologs in a single genome (S.K.H. and J.F.H., unpublished data). Earlier sequence-profiling analyses predicted that many families of TA systems are evolutionarily related to one another and that functional protein domains have been exchanged between different TA systems (Anantharaman and Aravind, 2003; Makarova et al., 2009; Smith and Magnuson, 2004). Our sequence-profiling analyses corroborate most of these results, correctly linking the structurally related RelE/YoeB toxins (Figure 1) and MazF/Kid/CcdB toxins (not shown). Although earlier studies also predicted homology between PhD, YefM, and some VapC-neutralizing antitoxins (Anantharaman and Aravind, 2003; McKinley and Magnuson, 2005), the similarity levels between these different families were statistically unconvincing in our sequence-profiling analyses. However, the crystal structure of the PhD-Doc complex reported in this paper (Table 1 and Figures 2 and 3) unambiguously proves this relationship, showing that the DNA-binding domain of PhD has the same fold as that of YefM. In addition, the crystal structures of YeeU presented in this paper establish that YeeU, which possesses antitoxin-like activity (Brown and Shaw, 2003), has a similar structure to RelE/YoeB-family toxins. This result suggests an evolutionary relationship between functionally antithetical YeeU-family antitoxins and RelE/YoeB-family toxins, even though they do not exhibit significant sequence similarity. Proteins from families related by statistically significant sequence or structural similarity were combined into sequence profiles to identify the final set of homologous families shown in Figure 1.

Experimental structure determination has proven to be a critical tool, not only in helping to elucidate the function of some TA systems (Kamada and Hanaoka, 2005; Kamada et al., 2003; Mattison et al., 2006; Miallau et al., 2009; Takagi et al., 2005) but also in confirming evolutionary relationships linking apparently disparate systems. In addition to establishing clear structural similarity between proteins exhibiting weak or

undetectable sequence similarity to their counterparts in other bacteria, as cited above, earlier structural results have confirmed the prediction that RelE toxins could be neutralized by antitoxins from unrelated families (Anantharaman and Aravind, 2003; Makarova et al., 2009) (Figure 1). *M. tuberculosis* RelE (Rv2866) forms a complex with a YefM-like antitoxin (*M. tuberculosis* RelB, Rv2865, Protein Data Bank [PDB] ID code 3G5O), whereas the *E. coli* RelE is neutralized by an antitoxin (*E. coli* RelB, PDB ID code 2K29) with a completely different fold (Li et al., 2008, 2009; Takagi et al., 2005). The structure of Phd presented in this paper (Table 1 and Figures 2 and 3) confirms a prediction that the YefM-like antitoxin fold has been adapted to neutralize toxins with different folds (Anantharaman and Aravind, 2003; Makarova et al., 2009). The structures of YeeU presented in this paper (Table 1) extend the impact of structural results on TA biology in two new ways. First, they demonstrate that some homologies between TA systems have not been detected using existing sequence-profiling methods (Altschul et al., 1997). Second, they demonstrate that the component of the YeeUV (W) system with antitoxin activity (Brown and Shaw, 2003) has significant structural similarity to the RelE/YoeB toxin fold. This observation, which represents the first report of a structural relationship between toxin and antitoxin species, shows that a single nucleic acid-binding fold has been adapted to perform both growth-inhibiting toxin functions and an expression-regulating antitoxin function. Therefore, our results on YeeU highlight the importance of experimental structure determination in elucidating the complex evolutionary relationships between components of different TA systems.

Crystal Structure of the Complete Phd-Doc Complex

Our crystal structure of the Phd-Doc complex contains a 2:2 Phd-Doc heterotetramer (Figure 2 and Table 2). Each Doc toxin is bound to a single Phd antitoxin, and the resulting Phd-Doc complex dimerizes based exclusively on contacts between two Phd molecules. Several analytical methods indicate that Phd-Doc tends to adopt a heterogeneous aggregation state in solution (our data and Gazit and Sauer, 1999a) but that the 2:2 oligomer is likely to be the dominant species in our Phd-Doc preparation. Coomassie blue staining of SDS-PAGE gels (e.g., as shown in the inset in Figure S1 available online) shows a roughly equal stoichiometry of Phd and Doc in the stock produced by our two-step purification procedure, which involves Ni-NTA affinity chromatography of His_6-tagged Doc followed by preparative gel-filtration chromatography. Analytical gel-filtration chromatography of this preparation monitored using inline static-light-scattering and refractive-index detectors (Figure S1) shows heterogeneity in oligomeric state, including some higher-order oligomers and a minor trailing shoulder likely containing a 2:1 Phd-Doc complex (based on its measured molecular weight of ~30 kDa versus 30,839 kDa predicted). However, the bulk of the protein mass is observed in a larger complex with mean molecular weight of ~37 kDa, which is consistent with an equilibrium between 2:2 and 2:1 Phd-Doc complexes after ~10-fold dilution of the crystallization stock coming through the gel-filtration column. Therefore, the undiluted stock is likely to be dominated by the larger oligomer observed in our crystal structure. Nonetheless, the heterogeneous aggregation state of Phd-Doc and its smaller 2:1 complex may have biological significance in modulating the dynamics of toxin activation, as discussed in Supplemental Information.

In contrast to the previously reported $Phd^{52–73}$-Doc structure (Garcia-Pino et al., 2008), which contained only the C-terminal neutralization domain of Phd, our complex structure contains the full-length Phd-Doc complex (Figure 2) and shows unambiguous electron density for 72 of the 73 residues in Phd, with only its N-terminal methionine being disordered. This structure confirms the inference that Phd has a modular structure (McKinley and Magnuson, 2005; Smith and Magnuson, 2004) because its N-terminal DNA-binding domain does not make any noncovalent packing interactions with its C-terminal neutralization domain. The structure shows no significant conformational differences in Doc compared to the previously reported structure in complex with $Phd^{52–73}$ (Garcia-Pino et al., 2008). Our structure shows electron density for 123 (chains C and D) or 124 residues (chains A and B) out of 126 total in Doc; the previously reported structure similarly has electron density for 123 residues, with 2 or 3 C-terminal residues and the hexahistidine tag being disordered in the crystal lattice.

Doc is a helical-bundle protein composed of six α helices. The Doc fold has yet to be classified in the SCOP protein fold database (Murzin et al., 1995), but Doc exhibits structural similarity to the Fic protein (Garcia-Pino et al., 2008) and AvrB, a secreted bacterial toxin (Kinch et al., 2009). Both of these homologous proteins interact with nucleotides (Table 1). Two residues essential for Doc activity (Magnuson and Yarmolinsky, 1998), His-66 and Asp-70, are positioned in a surface-exposed loop connecting α helices 3 and 4. There is clear evidence that the side chain of this histidine is mobile in our structure because it shows electron density for two conformations in all of the crystallographically independent subunits of Doc (data not shown). The substitution of this histidine for tyrosine does not significantly affect the structure, as superposition of our structure with that previously reported for the H66Y mutant of Doc (Garcia-Pino et al., 2008) reveals that the histidine and tyrosine side chains occupy the same physical location. Moreover, the two structures show no qualitative conformational difference (0.9 Å root-mean-square deviation [rmsd] for superposition of 123 Cα atoms). Our Doc structure has a spontaneously occurring F68S mutation in the same loop containing H66. Although this mutation does not significantly perturb backbone conformation compared to the previously reported structure with the wild-type phenylalanine residue at position 68, it may have been selected during plasmid propagation because it attenuates Doc toxicity. Such an effect would not be surprising, given the fact that the amino acids at the −2 (His-66) and +2 (Asp-70) positions in the same loop are essential for activity.

The structure of the N-terminal DNA-binding domain of Phd (Figure 2; Figure S1) has the following topology: β1 (residues 3–5) followed by kinked α helix, α1 (residues 6–11, 13–22), β2 (residues 26–29), β3 (residues 36–40), and a second kinked α helix, α2 (residues 41–62, 64–72). The three β strands of Phd form an antiparallel β sheet which makes a six-stranded β sheet via dimerization of the two Phd subunits (Figures 2 and 3). The bottom surface of the Phd N-terminal DNA-binding domain has an intense patch of positive electrostatic potential (Figure 2D) that is a common characteristic of DNA-binding proteins.

Table 1. Structural Similarity of Phd-Doc, HigA, and YeeU

Protein/Organism	PDB ID Code	Z Score	RMSD	Number Aligned[b]	Sequence Identity (%)	Dali Rank	Function	SCOP Family
Proteins with a Similar Structure to Doc								
Fic-domain-containing protein: *Bacteroides thetaiotaomicron*	3CUC	7.5	3.2	116 (268)	16	11	Function not determined[a]	Fic-like
AvrB: *Pseudomonas syringae*	1NH1	7.4	3.6	110 (290)	11	12	Membrane-associated toxin that targets host immune resistance proteins	Antivirulence factor (fold and family are the same)
Fic: *Neisseria meningitidis*	2G03	6.7	3.1	105 (177)	15	17	Function not determined[a]	Fic-like
Fic: *Helicobacter pylori*	2F6S	6.5	3.1	106 (180)	13	20	Function not determined[a]	Fic-like
Cytotoxin L: *Clostridium sordellii*	2VKH	4.4	4.6	79 (533)	6	63	"Lethal toxin" that targets Rho GTPases of the mammalian host	Nucleotide-diphospho-sugar transferases
δ-endotoxin CryIIIA: *Bacillus thuringiensis*	1DLC	2.4	5.0	84 (584)	12		Pore-forming toxin that disrupts gut epithelia membranes	Toxins' membrane translocation domains (N-terminal domain)
Proteins with a Similar Structure to Phd								
YefM (Rv2865): *M. tuberculosis*	3G5O	6.3	3.1	58 (92)	21	1	Antitoxin protein that neutralizes RNA-degrading RelE toxin	YefM-like
YefM (Rv3357): *M. tuberculosis*	3CTO	7.3	2.4	55 (65)	25	3	Antitoxin protein that neutralizes RNA-degrading YoeB toxin	YefM-like
YefM: *E. coli*	2A6Q	7.3	1.6	52 (58)	25	5	Antitoxin protein that neutralizes RNA-degrading YoeB toxin	YefM-like
NE2111: *Nitrosomonas europaea*	2ODK	6.6	1.7	49 (50)	27	15	Putative antitoxin protein of predicted YefM-FitB TA system	YefM-like
Proteins with a Similar Structure to YeeU								
YeeU: *Shigella flexneri*	2INW	20.7	0.8	104 (116)	93	3	Putative antitoxin protein of the YeeU-YeeV TA system	Profilin-like
YfjZ: *E. coli*	2EA9	17.5	1.2	99 (103)	62	5	Putative antitoxin of the predicted YpjF-YfjZ TA system	Profilin-like
RelE: *Pyrococcus horikoshii*	1WMI	4.0	3.5	69 (88)	7	182	RNA-degrading toxin of RelBE TA system	RelE-like
RelE: *E. coli*	2KC8	3.4	3.6	67 (95)	7	316	RNA-degrading toxin of RelBE TA system	(Pending)
RelE: *M. jannaschii*	3BPQ	2.7	4.1	61 (85)	7	421	RNA-degrading toxin of RelBE TA system	(Pending)
RelE: *M. tuberculosis*	3G5O	2.9	3.5	62 (81)	10	434	RNA-degrading toxin of YefM-RelE TA system	(Pending)

Table 1. *Continued*

Protein/Organism	PDB ID Code	Z Score	RMSD	Number Aligned[b]	Sequence Identity (%)	Dali Rank	Function	SCOP Family
YoeB: *E. coli*	2A6S	3.0	3.2	61 (84)	7	436	RNA-degrading toxin of YefM-YoeB TA system	RelE-like
Proteins with a Similar Structure to HigA								
YbaQ: *E. coli*	2EBY	13.2	2.7	89 (102)	29	3	Putative HTH-type transcriptional regulator	(Pending)
Putative antidote protein: *Nostoc punctiforme* PCC 73102	3CEC	12.9	5.1	88 (91)	26	5	Putative antidote protein of TA system	(Pending)
DNA-binding domain of C2 repressor: *Salmonella* bacteriophage P22	1ADR	8.4	1.9	67 (76)	16	6	HTH-type transcriptional regulator	λ repressor-like DNA-binding domains
DNA-binding domain of C1 repressor: bacteriophage 434	1R69	8.1	1.6	62 (63)	18	10	HTH-type transcriptional regulator	λ repressor-like DNA-binding domains
E. coli MqsA antitoxin (YgiT/b3021)	3GN5	4.5	2.6	54 (132)	19	218	HTH-type transcriptional regulator	(Pending)

[a] Fic domains have been shown to mediate bacterial pathogenicity by adenylation of host-cell proteins.
[b] The number in parentheses indicates the total length of the similar structure.

Genetic studies have determined that the C-terminal domain of Phd (amino acids 52–73) is the minimal unit of Phd required for Doc inhibition (McKinley and Magnuson, 2005; Smith and Magnuson, 2004). Our structure, combined with that of Loris and coworkers (Garcia-Pino et al., 2008), explains the structural basis for this observation. The C terminus of Phd (residues 52–73) adopts a kinked α-helical conformation. Amino acids 54–62 are predominately hydrophobic and pack into a hydrophobic groove on Doc; the kink in the Phd helix allows charged amino acids in the distal portion of the C terminus to interact with charged residues on an adjacent face of Doc (Figures 2B, 2C, and 3C). Residues His-66 and Asp-70, which are required for Doc activity, are not occluded by binding of the Phd antitoxin (Figure 2B). As noted (Garcia-Pino et al., 2008), this observation suggests that Phd may inhibit Doc toxicity indirectly by making the complex so large that steric hindrance prevents Doc from binding to its target site on ribosomes. A similar inhibitory mechanism has previously been proposed for the RelBE TA complex (Takagi et al., 2005).

Homologs of Phd

The program Dali was used to search the Protein Data Bank for proteins with structural similarity to Phd (Table 1), and the top four results were all proteins annotated as antitoxins: the YefM antitoxin of the *E. coli* YefM-YoeB TA system (PDB ID code 2A6Q, Z score of 7.3 and 1.6 Å rmsd for alignment of 52 residues with 25% sequence identity) (Figures 3A and 3B); protein Rv3357 from *M. tuberculosis* (PDB ID code 3CTO, Z score of 7.3 and 2.4 Å rmsd for alignment of 55 residues with 25% sequence identity); protein NE211, a putative prevents host death (Phd) protein, from *Nitrosomonas europaea* (PDB ID code 2ODK, Z score of 6.6 and 1.7 Å rmsd for alignment of 49 residues with 27% sequence identity); and protein Rv2865 from *M. tuberculosis* (PDB ID code 3G5O, Z score of 6.3 and 3.1 Å rmsd for alignment of 58 residues with 21% sequence identity). The structures of NE211 and Rv3357 (Kumar et al., 2008) do not contain the cognate toxins, whereas the structure of *M. tuberculosis* Rv2865 antitoxin was determined as a complex with the Rv2866 toxin, which has an equivalent backbone fold to that of the RelE and YoeB toxins. The YefM and NE2111 proteins are classified by the SCOP database as having a YefM-like fold and, based on the high degree of structural similarity (Figures 3A and 3B), it is likely that the other three homologous antitoxins would also be classified as YefM-like folds. Sequence-profiling analyses had predicted that the Phd and YefM antitoxins are homologous to one another (Anantharaman and Aravind, 2003; McKinley and Magnuson, 2005); our crystal structure of Phd proves that this inference is correct.

The strong conservation of the N-terminal DNA-binding domain of these homologous antitoxins is consistent with its function in regulating expression of the corresponding TA complexes. Although repression of both Phd-Doc and YefM-YoeB transcription is enhanced by the binding of the complete TA complex to its operator (Kedzierska et al., 2007; Magnuson and Yarmolinsky, 1998), the minimal requirement for repression is a dimer of the conserved N-terminal DNA-binding domain (Gazit and Sauer, 1999b; Kedzierska et al., 2007; Smith and Magnuson, 2004). All four of the homologous antitoxins form

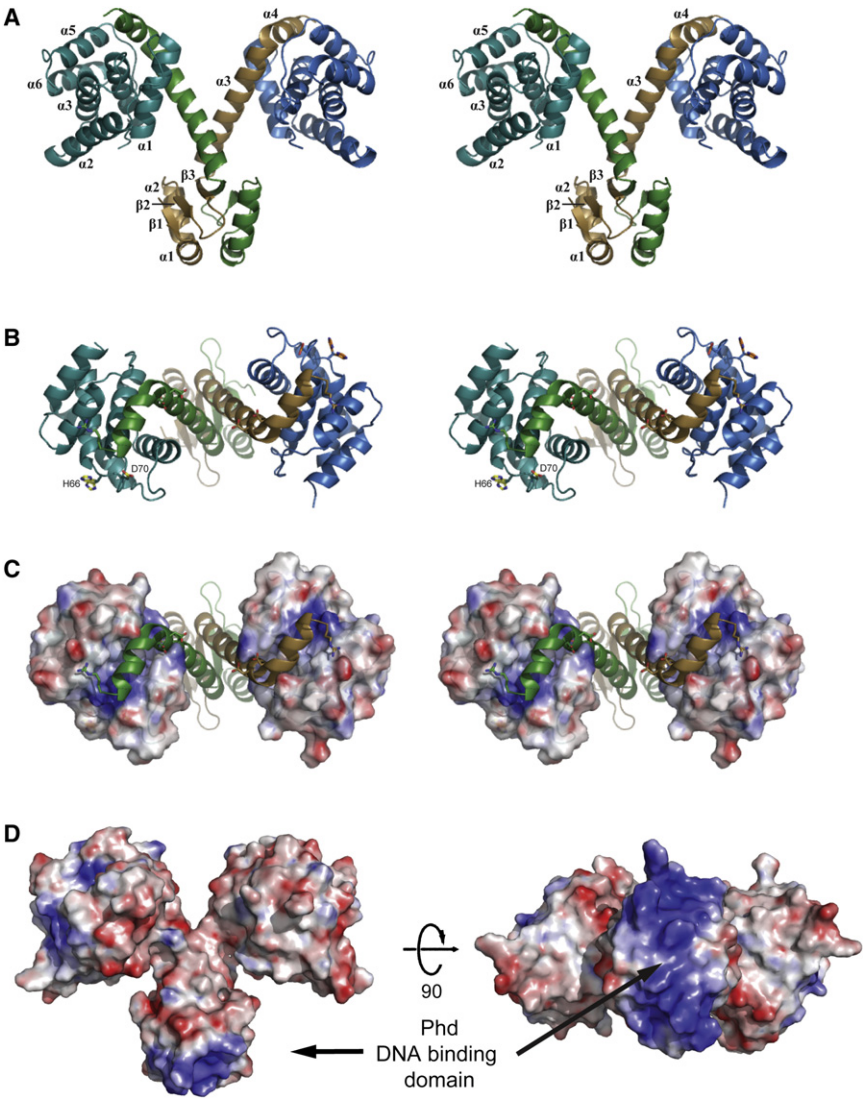

Figure 2. The Structure of the Heterotetrameric Phd-Doc Complex

(A) Stereo view of the 2:2 Phd-Doc complex. Phd molecules are colored green and brown, while Doc molecules are colored blue and dark teal.

(B) Another stereo view of the 2:2 Phd-Doc complex highlighting the Phd-Doc interactions (rotated 90° around a horizontal axis compared with the view in A). Charged residues in the Phd neutralization domain that interact with charged Doc residues are shown in stick representation. Residues implicated in Doc function (His-66, Asp-70) are colored yellow and orange for contrast and are shown in stick representation.

(C) Surface representation of Doc colored according to electrostatic potential, with blue and red, respectively, representing surface potentials of 5 kT and −5 kT in 100 mM salt (oriented as in B). Charged residues in the neutralization domain of Phd are shown in stick representation.

(D) Two views of the molecular surface of the Phd-Doc complex colored by electrostatic potential using the same parameters. The left panel is in the same orientation as (A), whereas the right panel is rotated 180° compared to the view in (B).

similar homodimer structures with at least 1200 Å^2 of solvent-accessible surface area per protomer buried in the intersubunit interface (1393 Å^2 for Phd, 1397 Å^2 for *E. coli* YefM, 1240 Å^2 for NE2111, 1333 Å^2 for Rv2865, and 1235 Å^2 for Rv3357) (Krissinel and Henrick, 2007). The critical elements for regulation of TA operon expression thus reside in the DNA-binding domain of the Phd/YefM antitoxins, explaining the conservation and proliferation of this domain in multiple TA subfamilies.

The Phd/YefM Fold Has Been Adapted for Neutralization of Structurally Unrelated Toxins

Sequence analysis studies have suggested that gene duplication and recombination events fused the Phd DNA-binding domain with the neutralization domain of structurally distinct antitoxins, thus creating new chimeric TA systems (McKinley and Magnuson, 2005; Smith and Magnuson, 2004). Our Phd-Doc crystal structure supports the hypothesis that antitoxin modules have been swapped between structurally and functionally distinct toxin systems in the course of bacterial evolution. Whereas the N-terminal DNA-binding module is conserved in all of the antitoxins related to PhD and YefM, the toxin neutralization domain varies in both sequence and length (Figure S2).

These sequence differences presumably reflect evolutionary adaptations necessary for high-affinity interaction with structurally distinct toxins. The Doc toxin has an all-α-helical fold that differs from the YoeB/RelE fold, which has a central β sheet flanked by α helices (Figures 3D). There is no structure available for NE2112, but sequence analyses suggest that this protein has a fold related to that of the FitB/VapC toxin family, which is different from that of either Doc or YoeB/RelE. A PSI-BLAST search of the Protein Data Bank reveals that NE2112 has 32% identity to FitB from *Neisseria gonorrhoeae* (PDB ID code 2H1C) (Mattison et al., 2006), 25% identity to *M. tuberculosis* VapC-5 (protein Rv0627, PDB ID code 3DBO), and 20% identity with another VapC-family toxin from *M. tuberculosis* (protein Rv0301, PDB ID code 3H87). Secondary-structure prediction using the PredictProtein server (Rost et al., 2004) indicates a high probability that NE2112 has an equivalent α/β/α secondary structural organization to these proteins (data not shown). Antitoxins homologous to Phd thus neutralize toxins with at least three different folds (Figure 1). The structural differences between the Doc, RelE/YoeB, and NE2112 toxins lead to substantial differences in their structural interactions with the neutralization domains of the corresponding Phd/YefM-like antitoxins, as detailed in Supplemental Information.

Homologs of Doc

An evolutionary relationship between the Doc toxin and the Fic family of proteins has recently been proposed based on

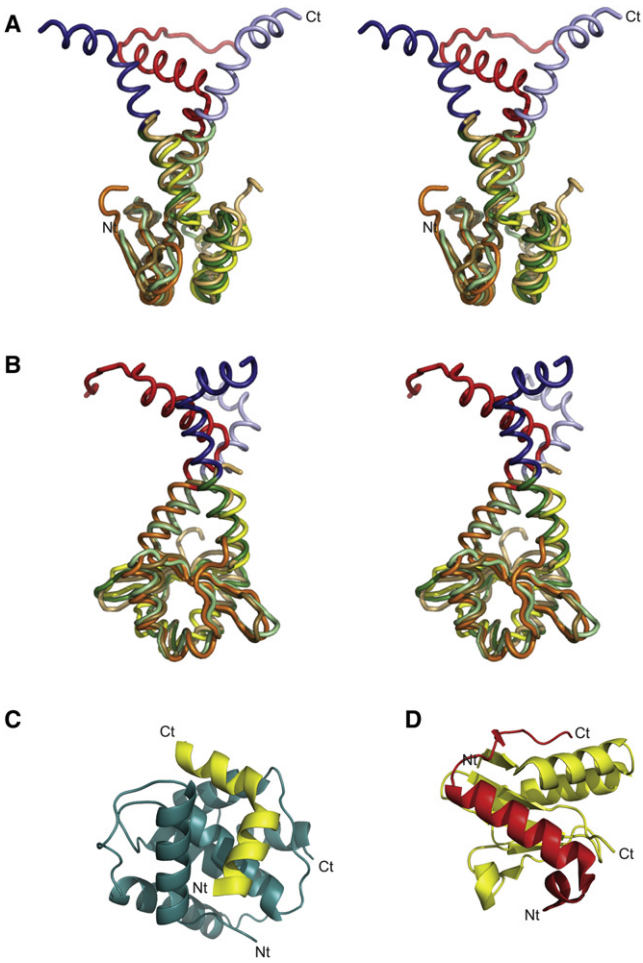

Figure 3. Homologous Phd/YefM/NE2111 Antitoxins Neutralize Toxins with Disparate Folds

(A and B) Stereo view of the superposition of Phd with *Ec*YefM and NE2111 antitoxins. In (A), Phd is in the same orientation as in Figure 2A, whereas in (B), the antitoxins are rotated by 90°. The DNA-binding domains are in green (Phd), yellow (*Ec*YefM), and orange (NE2111) while the toxin neutralization domains of Phd and *Ec*YefM are colored blue and red, respectively.

(C) The interaction of the Phd neutralization domain (in yellow, residues 52–73) with Doc (colored dark teal).

(D) Interaction of the *Ec*YefM neutralization domain (in red, residues 61–92) with YoeB (colored yellow).

sequence (Figure 4A) and structural (Figures 4B and 4C) similarity (Garcia-Pino et al., 2008; Kinch et al., 2009). Whereas early studies suggested that Fic proteins function in bacterial cell division (Kawamukai et al., 1988; Komano et al., 1991), recent work has demonstrated that pathogenic bacteria export Fic-domain-containing proteins into the cytosol of host cells, where they act as toxins modifying and inactivating critical host-cell proteins (Yarbrough et al., 2009). A bioinformatics study has proposed that the Fic domains share a common ancestor with Doc and AvrB, another secreted toxin involved in bacterial pathogenesis (Lee et al., 2004), and that these proteins constitute the "Fido" protein superfamily (Kinch et al., 2009).

A Dali search confirmed that the most closely related proteins to Doc (Table 1) are Fic-domain-containing proteins and *Pseudomonas syringae* AvrB (PDB ID code 1NH1) (Lee et al., 2004) (Figures 4B and 4C). This search also showed weaker but nonetheless significant structural similarity to domains from a number of substantially larger secreted bacterial toxins, including the "lethal toxin" from *Clostridium sordellii* (Table 1). These structural comparisons, which are discussed in greater depth in Supplemental Information, suggest complex evolutionary relationships between the growth-regulating toxins related to Doc and many different families of secreted toxins that kill eukaryotic target cells during bacterial pathogenesis.

Superimposing Doc with AvrB (Figures 4B and 4C) provides insight into possible functional features underlying the evolutionary relationships between proteins from different branches of the Fido-domain family. The structural similarity between these proteins spans most of the α-helical bundle formed by Doc (Z score of 7.4 and 3.6 Å rmsd for alignment of 110 residues with 11% sequence identity). AvrB has two domains, a smaller mixed-α/β domain and a larger α-helical bundle domain, separated by a substantial cleft. A mononucleotide-binding site in AvrB, located on the upper face of the α-helical bundle facing the cleft, mediates enzymatic phosphorylation of target proteins. The structural similarity between Doc and AvrB is restricted to the α-helical domain in AvrB, and Doc lacks the small domain that covers the mononucleotide-binding site in AvrB. This small domain presumably aids AvrB in catalyzing target protein phosphorylation using bound ATP but, if present in Doc, it would obscure His-66 and Asp-70 (Figures 4A and 4B), which have been proposed to interact with 16S rRNA when Doc binds to ribosomes. Mutations in either of these residues eliminate Doc toxicity (Magnuson and Yarmolinsky, 1998), and they have been hypothesized to contact rRNA based on the observation that Doc interaction with ribosomes is competitively inhibited by the aminoglycoside antibiotic hygromycin B (Liu et al., 2008), which binds directly to 16S rRNA near the decoding center of the ribosome (Brodersen et al., 2000).

Importantly, His-66 and Asp-70, the putative rRNA-binding residues in Doc, are conserved in other Fido-domain proteins, including AvrB (Kinch et al., 2009). In this protein, they are located proximal to the phosphates of its bound mononucleotide (Figures 4A and 4B). This observation, combined with the hypothesis that this region of Doc interacts with rRNA, provides a possible functional explanation for the likely common evolutionary ancestry of the secreted and growth-regulating toxins from different branches of the Fido-domain family (Kinch et al., 2009). Specifically, we propose that these proteins employ their mutually conserved surface to interact with different nucleic acid ligands and substrates. In AvrB, the conserved residues on this surface contribute to recognition of the ribonucleotide ATP and also likely catalysis of transfer of its γ-phosphate group to target host-cell proteins. The homologous Fic proteins are believed to use an overlapping active site to catalyze covalent modification of target proteins with AMP, again using an ATP substrate (Kinch et al., 2009). In Doc, the equivalent residues presumably mediate interaction with equivalent chemical moieties in rRNA, which of course is a polymer of ribonucleotides. Although Doc is not known to have catalytic activity, it conceivably could contribute to a ribonucleotide-related activity as part of some supramolecular complex.

Table 2. Phd-Doc, YeeU, and HigA Refinement Statistics

	Bacteriophage P1 Phd-Doc	*E. coli CFT073* HigA	*E. coli*YeeU	*S. flexneri* YeeU
Crystal Parameters				
Space group	$P2_12_12_1$	C2	$P2_1$	$P2_12_12_1$
Unit cell parameters (Å) at 100K	95.9, 111.3, 118.8 (90°, 90°, 90°)	90.5, 26.4, 39.5 (90°, 91.5°, 90°)	54.3, 45.3, 60.2 (90°, 109°, 90°)	31.5, 74.0, 110.7 (90°, 90°, 90°)
Data quality				
Resolution (Å)	40.0–2.7	30.0–1.63	40.0–2.1	19.42–1.5
R_{sym} [$I \geq -3\sigma(I)$] (%)	13.8	23.7	5.5	7.3
Mean redundancy	8.2	5.75	2.27	7.00
Completeness (all) (%)	91.2	98.5	99.1	97.1
($I \geq \sigma_I$) (%)	80.5	85.8	91.0	79.8
Mean I/σI	18.2	17.57	15.6	24.9
Refinement Residuals				
R_{free} (%)	26.7	22.5	25.3	25.0
R_{work} (%)	21.7	18.4	22.0	22.5
Model quality				
Rmsd bond lengths (Å)	0.007	0.005	0.006	0.006
Rmsd bond angles (°)	0.910	1.01	1.3	1.40
Ramachandran plot				
Core	94.9	95.2	91.0	90.4
Allowed	4.9	4.8	9.0	9.6
Generously allowed	0.1	—	—	—
Model contents				
Protein residues	Doc: A1–124, B1–124, C1–123, D1–123 PhD: E2–73, F2–73, G2–73, H2–73	A1–94	A16–124,[a] B15–118	A4–120, B4–119
Waters	95	96	82	256
Cl	1	—	1	—
PO_4	4	—	—	1
Mg	—	—	2	—
Glycerol	3	—	1	—
PDB ID code	3KH2	2ICT	2H28	2INW

[a] Residues 123 and 124 of *Ec*YeeU chain A belong to the affinity tag.

Crystal Structure of HigA

The HigBA complex from *E. coli* CFT073 was subjected to extensive crystallization screening, but the resulting crystals contained only the HigA antitoxin. HigA is classified by the SCOP database as having a λ repressor-like DNA-binding domain fold, and the HigA structure (Figure 5) shows a canonical helix-turn-helix (HTH) DNA-binding fold consisting of five α helices (α1–α5 at residues 9–20, 24–31, 35–43, 50–59, and 64–80, respectively). The most relevant results from a Dali search were an *E. coli* DNA-binding protein, a putative antitoxin from a *Nostoc punctiforme* TA system, bacteriophage HTH-type transcriptional regulators, and the *E. coli* MqsA antitoxin (Table 1).

Sequence-profiling studies suggest that HigB, the cognate toxin of the HigA antitoxin, is evolutionarily related to the RelE/YoeB toxin family and shares the same protein fold (Pandey and Gerdes, 2005). The HigA structure therefore confirms the inference that toxins from this single structural family are neutralized by antitoxins from at least three different fold families, that is, the HTH family represented by HigA, the nonglobular all-α-helical family represented by *Ph*RelB, and the YefM-like family (Figure 1). These three antitoxin families all have members with experimentally characterized structures, including the Phd and HigA structures presented in this paper (Figures 2, 3, and 5).

The genes encoding HigBA have a different organization from most TA systems, because the toxin precedes the antitoxin gene and both genes have their own promoters. A similar organization is shared by the genes encoding the MqsR-MsqA TA system, whose structure has recently been solved (Brown et al., 2009). Notably, the C-terminal DNA-binding domain of MqsA has an HTH fold that is structurally similar to the N-terminal DNA-binding domain of HigA (Figure 5B). The MqsR toxin has a RelE/YoeB-like fold, providing additional evidence that

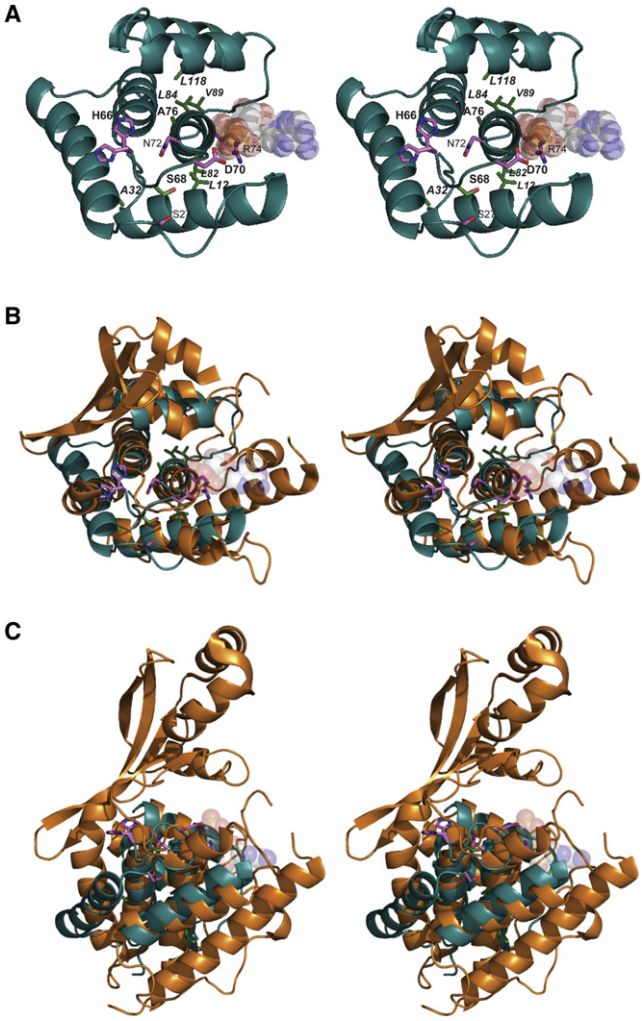

Figure 4. Structural Similarity of Doc to the Secreted Toxin AvrB

(A) Stereo view of the putative Doc active site. Residues conserved among Fido domains (Kinch et al., 2009) are colored magenta. Additional residues identified by Magnuson and Yarmolinsky (1998) that effect Doc activity are colored green, as is the F68S mutation present in our crystal structure. Mutations at sites labeled in bold text greatly attenuate the toxicity of Doc while interfering (italics) or not interfering (nonitalics) with its regulatory activity. The F68S mutation and additional sites that are conserved among Fido domains are labeled in plain text. Structural alignment of AvrB (B and C) shows the residues conserved among Fido domains are proximal to its bound ADP molecule (shown in transparent space-filling representation).

(B) Stereo pair in the same orientation as (A) showing superposition of Doc (dark teal) with AvrB (orange). The small domain in AvrB covering its mononucleotide-binding site has been omitted to improve clarity.

(C) Stereo pair showing a different view of a superposition of the full AvrB structure with Doc.

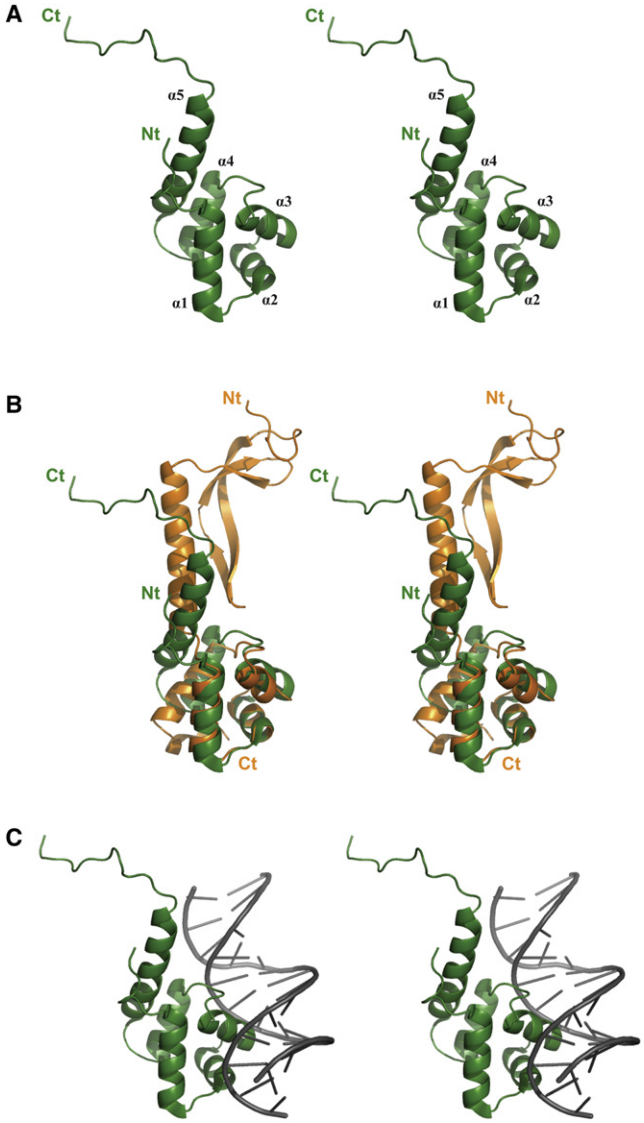

Figure 5. Structure of the HigA Antitoxin and Comparison with the MqsA Antitoxin

(A) Stereo view of the *E. coli* CFT073 HigA antitoxin. Although HigA neutralizes a toxin that is homologous to YoeB, it is structurally unrelated to the YefM antitoxin that neutralizes YoeB (see Figure 1).

(B) Stereo view of superimposed HigA and MqsA antitoxins. HigA and MqsA have structurally similar HTH DNA-binding domains but structurally dissimilar neutralization domains, even though they inhibit structurally homologous RelE/YoeB-family toxins. Therefore, RelE/YoeB-family toxins are neutralized by antitoxins from at least three fold families (YefM-like, HigA, and MqsA).

(C) Stereo view of a model of the HigA antitoxin in complex with DNA generated by superimposing HigA on the structure of the P22 c2 repressor protein in complex with DNA (PDB ID code 2R1J).

RelE/YoeB-family toxins are neutralized by antitoxins belonging to distinct fold families. In fact, although the DNA-binding domains of HigA and MqsA share the same fold, their neutralization domains have different folds. The N-terminal neutralization domain of MqsA consists of a single α helix plus three β strands, which form a continuous β sheet with the core β sheet in MqsR that is shared by all RelE/YoeB-like toxin family members. In contrast, the C-terminal neutralization domain of HigA is composed of an α helix and a loop but does not have any β structure (Figure 5A). Given this structural difference, as well as the different order in the polypeptide chain of their neutralization versus DNA-binding domains, the HigA and MqsA antitoxins themselves have significantly different structures even though they share one structural domain. Therefore, RelE/YoeB-family

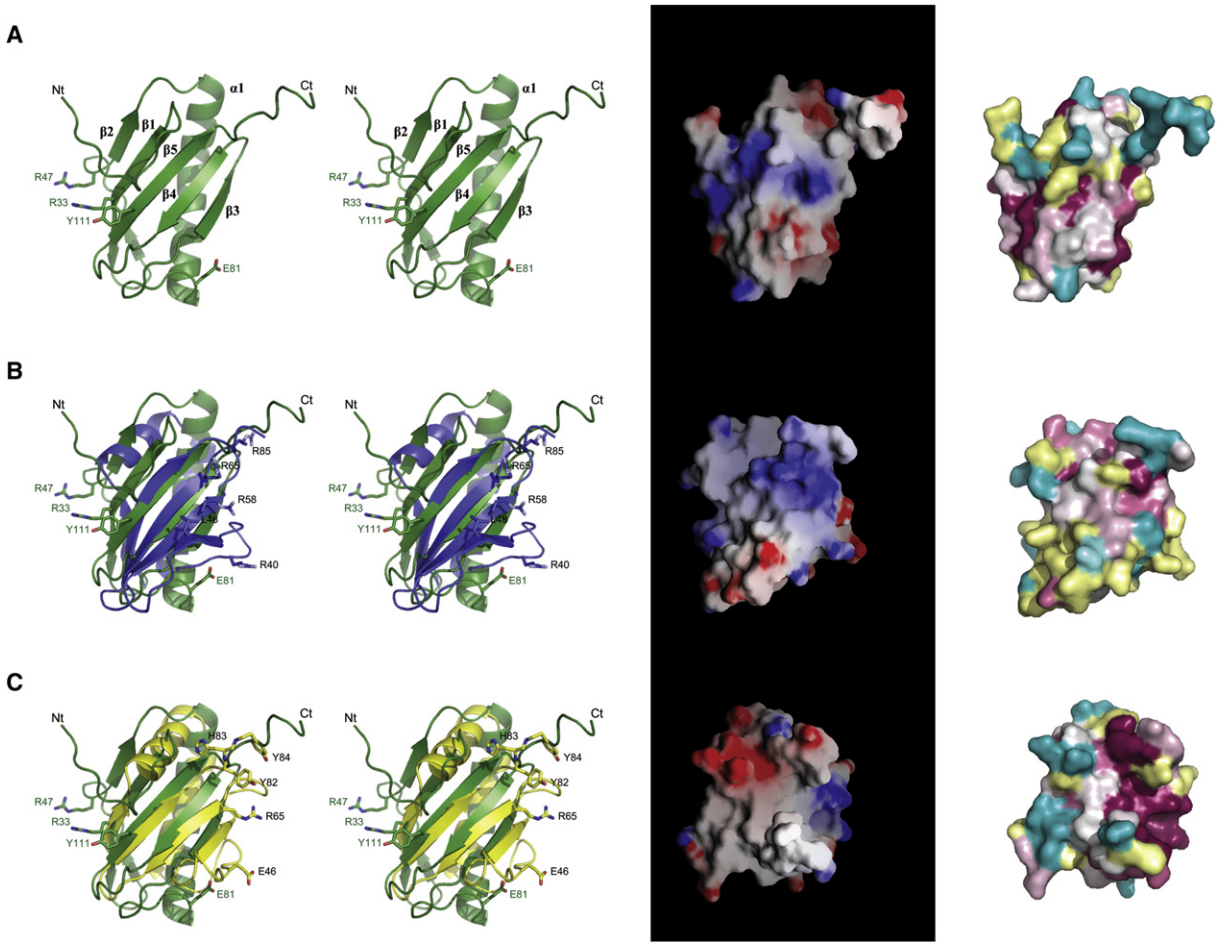

Figure 6. Comparison of the YeeU Antitoxin Structure to Related Structures

(A) The *Ec*YeeU structure. The left side shows a YeeU stereopair with putative functional residues labeled and shown in stick representation. The middle panel shows the electrostatic surface potential of YeeU, with blue and red, respectively, representing surface potentials of 9 kT and −6.5 kT in 100 mM salt. The panel on the right shows a surface representation of *Ec*YeeU colored according to sequence conservation using ConSurf (Landau et al., 2005) with a set of 20 YeeU homologs (including *E. coli* YafW and YfjZ) aligned by Clustal W (Larkin et al., 2007). Burgundy indicates a high degree of conservation whereas teal represents regions of variable sequence. Yellow indicates regions where degree of conservation could not be assigned with confidence.

(B) Stereo pair of *Ec*YeeU superimposed on *Ph*RelE. Residues known to be involved in *Ph*RelE function are labeled and shown in stick representation. The middle and right panels show the molecular surface of *Ph*RelE colored according to electrostatic surface potential and sequence conservation, respectively, using the same parameters as for *Ec*YeeU.

(C) Stereo pair of *Ec*YeeU superimposed on *Ec*YoeB. Residues known to be involved in *Ec*YoeB function are labeled and shown in stick representation. The middle and right panels show the molecular surface of *Ec*YoeB colored according to electrostatic surface potential and sequence conservation, respectively, using the same parameters as for *Ec*YeeU.

toxins are neutralized by antitoxins from at least four distinct fold families.

Crystal Structures of YeeU

YeeU is a single-domain protein with a core comprising a noncontinuous five-stranded antiparallel β sheet (Figure 6A and Figure S3). The topology of YeeU is as follows: β1 (residues 29–37), β2 (residues 40–42, 48–51), α1 (residues 56–79), β3 (residues 90–94), β4 (residues 97–102), and β5 (residues 109–116). A kinked α helix is inserted between strands β2 and β3, and it packs into a cavity on the back of the twisted β sheet. Strand β2 is interrupted by a single turn of a 3/10 helix. The *Ec*YeeU and *Sf*YeeU structures are highly similar (Z score of 20.7 and 0.8 Å rmsd for alignment of 105 residues), consistent with the 92% sequence identity between these proteins. (The *Ec*YeeU structure is used for the analyses reported in this paper.)

Structural Similarity of the YeeU Antitoxin to the Toxins RelE and YoeB

The YeeUV TA system was identified based on a bioinformatics analysis of the *E. coli* K12 genome for genes fulfilling several standard criteria for TA systems (Brown and Shaw, 2003). Experimental follow-up studies showed that YeeU suppresses the toxicity of YeeV but only when expressed from a single plasmid that contained the two genes in the same operon organization found in the *E. coli* chromosome, that is, separated by a 68 base pair intergenic untranslated region (UTR). The absence of YeeV expression from a plasmid with this structure led to the

conclusion that YeeU acts as a transcription factor or translation factor attenuating YeeV expression by interaction with this intergenic UTR (Brown and Shaw, 2003). This regulatory paradigm, which does not involve a direct physical interaction between the YeeU antitoxin and YeeV toxin, is fundamentally different from that of the other well-characterized bacterial TA systems. *E. coli* K12 encodes three additional proteins with strong amino acid sequence similarity to YeeU: YafW (62% identical), YfjZ (66% identical), and YagB (63% identical). Crystal and NMR structures of YfjZ confirm that it has the same fold as YeeU (PDB ID codes 2EA9 and 2JN7). The genes encoding YafW and YfjZ are upstream of genes encoding proteins homologous to YeeV (although these putative operons lack any equivalent of the downstream *yeeW* gene of unknown function found in the *yeeUVW* operon). YafW and YfjZ have both been demonstrated to suppress the toxicity of the downstream YeeU homologs encoded in their respective operons (Brown and Shaw, 2003), confirming that YeeU-family proteins generally have antitoxin activity.

A Dali search was used to generate clues concerning YeeU function (Table 1). The structurally similar proteins identified in this search include many with unknown functions as well as some functioning in transcriptional regulation (e.g., *E. coli* TyrR, PDB ID code 2JHE). The most striking result was the revelation that YeeU has the same core fold as the YoeB (Kamada and Hanaoka, 2005) and RelE (Li et al., 2009; Takagi et al., 2005) nucleic acid-interacting toxins. The highest degree of structural similarity to a known toxin is to the RelE toxin from *Pyrococcus horikoshii* (PDB ID code 1WMI, Z score of 4.0 and 3.5 Å rmsd for the alignment of 69 residues with 7% sequence identity) (Figure 6B). However, there is also significant similarity to the RelE toxins from *E. coli*, *M. tuberculosis*, and *Methanococcus jannaschii* and to YoeB from *E. coli* (PDB ID code 2A6S, Z score of 3.0 and 3.2 Å rmsd for the alignment of 61 residues with 7% sequence identity) (Figure 6C). In all of these proteins, the three-stranded β sheet and flanking α helix that form the structural core of YeeU (strands β3–5 and helix α1) align with equivalent secondary structural elements that occur with identical topology in the RelE/YoeB-family toxins (Figure 6). The structural differences in these toxins compared to YeeU are all limited to secondary structural elements on the edges of the central three-stranded β sheet (which cause YeeU and RelE/YoeB to be assigned different SCOP families). Structural elaborations of this kind are routine in the course of protein evolution (Andreeva and Murzin, 2006) and are consistent with the hypothesis that the likely nucleic acid-binding antitoxin YeeU could share a common evolutionary ancestry with nucleic acid-binding toxins from the RelE/YoeB family.

YeeU May Bind Nucleic Acids at a Homologous Site but Lacks Catalytic Residues from the Toxins

Previous studies have documented the structural similarity of RelE and YoeB to the microbial RNases barnase and RNase Sa (Kamada and Hanaoka, 2005; Takagi et al., 2005), as shown in Figure S6 and reviewed briefly in Supplemental Information. RelE has high-level RNase activity that mediates its cytotoxicity (Christensen and Gerdes, 2003; Pedersen et al., 2003). Whereas YoeB had demonstrated weak RNase activity in vitro (Kamada and Hanaoka, 2005; Zhang and Inouye, 2009), its cytotoxicity appears to be mediated primarily by noncovalent interaction with 50S ribosomal subunits which blocks translation initiation (Zhang and Inouye, 2009). All four of these proteins are believed to bind target RNAs at an equivalent region on the exposed surface of the homologous β sheets forming the structural core of these domains (Figures 6B and 6C; Figure S6) (Kamada and Hanaoka, 2005; Li et al., 2009; Takagi et al., 2005). Whereas a cluster of likely RNA-interacting/hydrolyzing residues is strongly conserved at these sites within each individual functional protein family, these residues are generally not preserved between the different functional families (Figure S6). For example, although YoeB shares two of the four active-site residues conserved between barnase and RNase Sa, neither of these residues is found in the active site of RelE, which conserves just a single arginine residue at an equivalent site compared to YoeB and no residues compared to barnase or RNase Sa. (See Supplemental Information for more details.)

A similar pattern of intrafamily amino acid conservation is observed at the equivalent site on the surface of YeeU (Figure 6; Figures S5 and S6). This region of YeeU contains a series of residues that are either invariant (Glu-81, Val-90, Thr-91, Thr-98, Asp-102, and Ala-113) or strongly conserved (Gln-87, His-88, and Tyr-115) among 20 YeeU homologs (including YafW and YfjZ). A basic region of the protein surface immediately adjacent to this site shows the strongest conservation of any segment of YeeU (including residues Arg-33, Arg-47, Glu-81, and Tyr-111) (Figure 6A; Figure S5). The stringent conservation of so many charged and aromatic residues, which are overrepresented in functional DNA-binding sites (Ades and Sauer, 1995), is consistent with this region of YeeU mediating the functional regulatory interactions with the intergenic UTR from YeeUV operon. The structural similarity in this region between protein families with widely diverged functions, as well as the strong amino acid conservation within each family, are consistent with the hypothesis that this surface forms a versatile nucleic acid-binding site that has been adapted to mediate different kinds of nucleic acid interactions over the course of bacterial evolution. Further studies of the regulation of the expression of YeeV-family proteins by YeeU-family proteins will be required to critically evaluate this hypothesis.

Conclusion

Our results uncovered unanticipated structural similarity between the components of disparate bacterial TA systems, while also proving that earlier sequence-based predictions of such similarity were indeed correct. Our crystal structure of Phd definitively proves that there is homology in the DNA-binding domains of antitoxins neutralizing toxins from the Doc, RelE/YoeB, and FitB/VapC families, all three of which have different protein folds (Figure 1). Although the relationship between Phd and YefM was predicted from sequence-profiling studies (Anantharaman and Aravind, 2003; Smith and Magnuson, 2004), proof that a single DNA-binding module has been adapted for interaction with different toxin folds required multiple experimental structure determinations from many different groups. Recent structural data on RelE toxins have proven that multiple antitoxin folds are capable of neutralizing RelE/YoeB-family toxins (Kamada and Hanaoka, 2005; Li et al., 2008; Takagi et al., 2005). Our crystal structure of the HigA antitoxin extends

these results by establishing another antitoxin fold capable of neutralizing these toxins.

Likewise, our structural results reveal latent structural similarity between YeeU, which has an antitoxin-like activity, and RelE/YoeB-family toxins. Therefore, these proteins seem likely to share common evolutionary ancestry despite the absence of detectable sequence similarity. Comparison of the structure of YeeU to that of related toxin structures provides insight into the antitoxin-like activity of YeeU by showing that this nucleic acid-binding repressor has a similar fold to that of the nucleic acid-binding toxins. Further biochemical studies will be required to establish the exact mechanism by which YeeU suppresses YeeV toxicity.

Our results demonstrate how evolutionary insights can emerge from structure determination. Several of the relationships between different TA systems discussed above would likely have remained elusive in the absence of experimental structural determinations. Structural studies thus provide a powerful approach to uncovering new functional and evolutionary relationships between protein families.

EXPERIMENTAL PROCEDURES

Phylogenetic Analyses of Eubacterial TA Systems

PSI-BLAST profiles (Altschul et al., 1997) were created for a set of canonical toxin and antitoxin families in the CRSH database of proteins of likely equivalent function from 474 fully sequenced bacterial genomes (Clusters of Reciprocal Sequence Homologs; http://www.orthology.org; S.K.H. and J.F.H., unpublished data). These profiles were used to identify families with significant sequence similarity (e value < 10^{-3}), which were combined with each other and with other families with established structural similarity (Holm and Park, 2000) to construct a new PSI-BLAST profile. This profile was used to identify the final set of families in each group, according to the same significance criterion. Cladograms were reconstructed by the program MEGA 3.0 (Kumar et al., 2004) based on 100 bootstrap replicates using the UPGMA method (Legendre and Legendre, 1998) with default parameters.

Cloning, Expression, and Purification

The Phd-Doc complex was cloned into pET21 with an LEHHHHHH affinity tag at the C terminus of Doc. Sequencing of the Phd-Doc plasmid revealed that there were mutations in three residues in the complex (L17M and V39A in Phd and F68S in Doc). The relatively conservative Phd mutations occur at partially solvent-exposed sites near the Phd homodimer interface and are unlikely to alter its structure based on preservation of both protomer fold and homodimer interactions in the *Ec*YefM and NE2111 antitoxins (Figure 3A). The Doc mutation is discussed in the text. Full-length *Ec*YeeU and *Sf*YeeU were cloned in the same manner. The HigBA complex from *E. coli* CFT073 was cloned into pET28 with an MGSSHHHHHHSSGLVPRGS affinity tag at the N terminus of HigB. Recombinant proteins were expressed in *E. coli* BL21λ(DE3) using MJ9 minimal medium supplemented with selenomethionine (Jansson et al., 1996). The proteins were purified by Ni-NTA affinity chromatography followed by gel filtration in 100 mM NaCl, 5 mM DTT, 10 mM Tris (pH 7.5) (Benach et al., 2003). Phd-Doc, *Ec*YeeU, *Sf*YeeU, and HigBA are Northeast Structural Genomics Consortium targets ER385/386, ER304, SfR137, and ER389/390, respectively.

Protein Crystallization

Crystals of the Phd-Doc complex grew at 21°C in 3 days to maximum dimensions of 50 × 50 × 700 μm from 1+1 μl hanging-drop vapor-diffusion reactions with the complex at 10.8 mg/ml over a 1 ml reservoir containing 2250 mM NaCl, 100 mM NaH_2PO_4, 100 mM K_2HPO_4, 3% ethanol, 100 mM MES (pH 6.5). Crystals of HigA, *Ec*YeeU, and *Sf*YeeU were all grown in 1:1 microbatch reactions under paraffin oil at 20°C. HigA crystals grew in 1 day to maximum dimensions of 20 × 40 × 200 μm after mixing the HigBA complex at 0.6 mg/ml with 35% 1,6-hexanediol, 5 mM $MgSO_4$, 50 mM Tris (pH 8.5). *Ec*YeeU crystals grew in 3 days to maximum dimensions of 50 × 50 × 200 μm after mixing the protein at 2 mg/ml with 20% PEG 4K, 0.1 M $MgSO_4$, 0.1 M MOPS (pH 7.0). *Sf*YeeU crystals grew in 2 days to maximum dimensions of 50 × 50 × 150 μm after mixing the protein at 2.2 mg/ml with 20% PEG 20K, 0.1 M KH_2PO_4, 0.1 M MES (pH 6.0). HigA and *Sf*YeeU crystals were frozen directly in liquid propane without cryoprotection, whereas Phd-Doc and *Ec*YeeU crystals were cryoprotected for 1 min in the corresponding precipitant solution plus 15% glycerol.

Structure Determination Methods

Diffraction data from crystals at 100K were processed with DENZO and SCALEPACK (Otwinowski and Minor, 1997). Data for Phd-Doc and HigA were collected on beamline NE-CAT ID-4 at the Advanced Photon Source, whereas data for YeeU were collected on beamline X4A at the National Synchrotron Light Source. The complete Phd-Doc complex was solved by molecular replacement with the program COMO (Jogl et al., 2001) using as a search model the Doc subunit of the complex containing only the 21 residue neutralization domain of Phd (PDB ID code 3DD7). The model was built using Coot (Emsley and Cowtan, 2004) and refined with REFMAC (Murshudov et al., 1997) including TLS parameters. The structure of HigA at physiological pH was solved by molecular replacement with the program COMO (Jogl et al., 2001) using as a search model a previously determined HigA structure at low pH (PDB ID code 2ICP). The structures of *Ec*YeeU and *Sf*YeeU were solved using single-wavelength anomalous diffraction data. The program SOLVE (Terwilliger and Berendzen, 1999) found four selenium sites for *Ec*YeeU and two for *Sf*YeeU. The structures of HigA, *Ec*YeeU, and *Sf*YeeU models were built with O (Jones et al., 1991) and refined with CNS (Brunger et al., 1998), yielding excellent stereochemical parameters (Table 2).

Structure Superposition and Display

Figures were prepared with PyMOL (DeLano, 2002). Structural similarity searches were performed with Dali (Holm et al., 2008). Electrostatic surface potentials were calculated with GRASP (Nicholls et al., 1991) or UHBD (Davis et al., 1991). Solvent-accessible surface area was calculated with PISA (Krissinel and Henrick, 2007).

ACCESSION NUMBERS

Atomic coordinates and structure factors for the crystal structures of the Phd-Doc TA system from bacteriophage P1, the HigA antitoxin from *Escherichia coli* CFT073, and YeeU antitoxins from *E. coli* K12 and *Shigella flexneri* have been deposited in the Protein Data Bank under ID codes 3KH2, 2ICT, 2H28, and 2INW, respectively.

SUPPLEMENTAL INFORMATION

Supplemental Information includes six figures and Supplemental Experimental Procedures and can be found with this article online at doi:10.1016/j.str.2010.04.018.

ACKNOWLEDGMENTS

This work was supported by grants from the Protein Structure Initiative of the U.S. National Institutes of Health (GM62413 and GM074958). We thank J. Schwanoff and R. Abramowitz for support during synchrotron data collection and J. Benach and N.K. Karpowich for help with structure solution and refinement. Diffraction data were collected on beamline X4A at the National Synchrotron Light Source of Brookhaven National Laboratory and NE-CAT beamline ID-4 at the Advanced Photon Source of Argonne National Laboratory.

Received: December 12, 2009
Revised: March 22, 2010
Accepted: April 21, 2010
Published: August 10, 2010

REFERENCES

Ades, S.E., and Sauer, R.T. (1995). Specificity of minor-groove and major-groove interactions in a homeodomain-DNA complex. Biochemistry *34*, 14601–14608.

Altschul, S.F., Madden, T.L., Schaffer, A.A., Zhang, J., Zhang, Z., Miller, W., and Lipman, D.J. (1997). Gapped BLAST and PSI-BLAST: a new generation of protein database search programs. Nucleic Acids Res. *25*, 3389–3402.

Anantharaman, V., and Aravind, L. (2003). New connections in the prokaryotic toxin-antitoxin network: relationship with the eukaryotic nonsense-mediated RNA decay system. Genome Biol. *4*, R81.

Andreeva, A., and Murzin, A.G. (2006). Evolution of protein fold in the presence of functional constraints. Curr. Opin. Struct. Biol. *16*, 399–408.

Benach, J., Lee, I., Edstrom, W., Kuzin, A.P., Chiang, Y., Acton, T.B., Montelione, G.T., and Hunt, J.F. (2003). The 2.3-Å crystal structure of the shikimate 5-dehydrogenase orthologue YdiB from *Escherichia coli* suggests a novel catalytic environment for an NAD-dependent dehydrogenase. J. Biol. Chem. *278*, 19176–19182.

Brodersen, D.E., Clemons, W.M., Jr., Carter, A.P., Morgan-Warren, R.J., Wimberly, B.T., and Ramakrishnan, V. (2000). The structural basis for the action of the antibiotics tetracycline, pactamycin, and hygromycin B on the 30S ribosomal subunit. Cell *103*, 1143–1154.

Brown, J.M., and Shaw, K.J. (2003). A novel family of *Escherichia coli* toxin-antitoxin gene pairs. J. Bacteriol. *185*, 6600–6608.

Brown, B.L., Grigoriu, S., Kim, Y., Arruda, J.M., Davenport, A., Wood, T.K., Peti, W., and Page, R. (2009). Three dimensional structure of the MqsR:MqsA complex: a novel TA pair comprised of a toxin homologous to RelE and an antitoxin with unique properties. PLoS Pathog. *5*, e1000706.

Brunger, A.T., Adams, P.D., Clore, G.M., DeLano, W.L., Gros, P., Grosse-Kunstleve, R.W., Jiang, J.S., Kuszewski, J., Nilges, M., Pannu, N.S., et al. (1998). Crystallography & NMR system: a new software suite for macromolecular structure determination. Acta Crystallogr. D Biol. Crystallogr. *54*, 905–921.

Christensen, S.K., and Gerdes, K. (2003). RelE toxins from bacteria and Archaea cleave mRNAs on translating ribosomes, which are rescued by tmRNA. Mol. Microbiol. *48*, 1389–1400.

Christensen-Dalsgaard, M., and Gerdes, K. (2006). Two higBA loci in the *Vibrio cholerae* superintegron encode mRNA cleaving enzymes and can stabilize plasmids. Mol. Microbiol. *62*, 397–411.

Condon, C. (2006). Shutdown decay of mRNA. Mol. Microbiol. *61*, 573–583.

Dao-Thi, M.H., Van Melderen, L., De Genst, E., Buts, L., Ranquin, A., Wyns, L., and Loris, R. (2004). Crystallization of CcdB in complex with a GyrA fragment. Acta Crystallogr. D Biol. Crystallogr. *60*, 1132–1134.

Davis, M.E., Madura, J.D., Luty, B.A., and McCammon, J.A. (1991). Electrostatics and diffusion of molecules in solution: simulations with the University of Houston Brownian dynamics program. Comput. Phys. Commun. *62*, 187–197.

DeLano, W.L. (2002). The PyMOL Molecular Graphics System (San Carlos, CA: DeLano Scientific).

Emsley, P., and Cowtan, K. (2004). Coot: model-building tools for molecular graphics. Acta Crystallogr. D Biol. Crystallogr. *60*, 2126–2132.

Garcia-Pino, A., Christensen-Dalsgaard, M., Wyns, L., Yarmolinsky, M., Magnuson, R.D., Gerdes, K., and Loris, R. (2008). Doc of prophage P1 is inhibited by its antitoxin partner Phd through fold complementation. J. Biol. Chem. *283*, 30821–30827.

Gazit, E., and Sauer, R.T. (1999a). The Doc toxin and Phd antidote proteins of the bacteriophage P1 plasmid addiction system form a heterotrimeric complex. J. Biol. Chem. *274*, 16813–16818.

Gazit, E., and Sauer, R.T. (1999b). Stability and DNA binding of the Phd protein of the phage P1 plasmid addiction system. J. Biol. Chem. *274*, 2652–2657.

Hargreaves, D., Santos-Sierra, S., Giraldo, R., Sabariegos-Jareno, R., de la Cueva-Mendez, G., Boelens, R., Diaz-Orejas, R., and Rafferty, J.B. (2002). Structural and functional analysis of the Kid toxin protein from *E. coli* plasmid R1. Structure *10*, 1425–1433.

Holm, L., and Park, J. (2000). DaliLite workbench for protein structure comparison. Bioinformatics *16*, 566–567.

Holm, L., Kaariainen, S., Rosenstrom, P., and Schenkel, A. (2008). Searching protein structure databases with DaliLite v.3. Bioinformatics *24*, 2780–2781.

Hurley, J.M., and Woychik, N.A. (2009). Bacterial toxin HigB associates with ribosomes and mediates translation-dependent mRNA cleavage at A-rich sites. J. Biol. Chem. *284*, 18605–18613.

Jansson, M., Li, Y.C., Jendeberg, L., Anderson, S., Montelione, B.T., and Nilsson, B. (1996). High-level production of uniformly ^{15}N- and ^{13}C-enriched fusion proteins in *Escherichia coli*. J. Biomol. NMR *7*, 131–141.

Jogl, G., Tao, X., Xu, Y., and Tong, L. (2001). COMO: a program for combined molecular replacement. Acta Crystallogr. D Biol. Crystallogr. *57*, 1127–1134.

Jones, T.A., Zou, J.Y., Cowan, S.W., and Kjeldgaard, M. (1991). Improved methods for building protein models in electron density maps and the location of errors in these models. Acta Crystallogr. A *47*, 110–119.

Kamada, K., and Hanaoka, F. (2005). Conformational change in the catalytic site of the ribonuclease YoeB toxin by YefM antitoxin. Mol. Cell *19*, 497–509.

Kamada, K., Hanaoka, F., and Burley, S.K. (2003). Crystal structure of the MazE/MazF complex: molecular bases of antidote-toxin recognition. Mol. Cell *11*, 875–884.

Kamphuis, M.B., Bonvin, A.M., Monti, M.C., Lemonnier, M., Munoz-Gomez, A., van den Heuvel, R.H., Diaz-Orejas, R., and Boelens, R. (2006). Model for RNA binding and the catalytic site of the RNase Kid of the bacterial parD toxin-antitoxin system. J. Mol. Biol. *357*, 115–126.

Kawamukai, M., Matsuda, H., Fujii, W., Nishida, T., Izumoto, Y., Himeno, M., Utsumi, R., and Komano, T. (1988). Cloning of the fic-1 gene involved in cell filamentation induced by cyclic AMP and construction of a delta fic *Escherichia coli* strain. J. Bacteriol. *170*, 3864–3869.

Kedzierska, B., Lian, L.Y., and Hayes, F. (2007). Toxin-antitoxin regulation: bimodal interaction of YefM-YoeB with paired DNA palindromes exerts transcriptional autorepression. Nucleic Acids Res. *35*, 325–339.

Kinch, L.N., Yarbrough, M.L., Orth, K., and Grishin, N.V. (2009). Fido, a novel AMPylation domain common to Fic, Doc, and AvrB. PLoS One *4*, e5818.

Komano, T., Utsumi, R., and Kawamukai, M. (1991). Functional analysis of the fic gene involved in regulation of cell division. Res. Microbiol. *142*, 269–277.

Krissinel, E., and Henrick, K. (2007). Inference of macromolecular assemblies from crystalline state. J. Mol. Biol. *372*, 774–797.

Kumar, S., Tamura, K., and Nei, M. (2004). MEGA3: integrated software for Molecular Evolutionary Genetics Analysis and sequence alignment. Brief. Bioinform. *5*, 150–163.

Kumar, P., Issac, B., Dodson, E.J., Turkenburg, J.P., and Mande, S.C. (2008). Crystal structure of *Mycobacterium tuberculosis* YefM antitoxin reveals that it is not an intrinsically unstructured protein. J. Mol. Biol. *383*, 482–493.

Landau, M., Mayrose, I., Rosenberg, Y., Glaser, F., Martz, E., Pupko, T., and Ben-Tal, N. (2005). ConSurf 2005: the projection of evolutionary conservation scores of residues on protein structures. Nucleic Acids Res. *33*, W299–W302.

Larkin, M.A., Blackshields, G., Brown, N.P., Chenna, R., McGettigan, P.A., McWilliam, H., Valentin, F., Wallace, I.M., Wilm, A., Lopez, R., et al. (2007). Clustal W and Clustal X version 2. Bioinformatics *23*, 2947–2948.

Lee, C.C., Wood, M.D., Ng, K., Andersen, C.B., Liu, Y., Luginbuhl, P., Spraggon, G., and Katagiri, F. (2004). Crystal structure of the type III effector AvrB from *Pseudomonas syringae*. Structure *12*, 487–494.

Legendre, P., and Legendre, L. (1998). Numerical Ecology (Amsterdam: Elsevier Science).

Li, G.Y., Zhang, Y., Inouye, M., and Ikura, M. (2008). Structural mechanism of transcriptional autorepression of the *Escherichia coli* RelB/RelE antitoxin/toxin module. J. Mol. Biol. *380*, 107–119.

Li, G.Y., Zhang, Y., Inouye, M., and Ikura, M. (2009). Inhibitory mechanism of *Escherichia coli* RelE-RelB toxin-antitoxin module involves a helix displacement near an mRNA interferase active site. J. Biol. Chem. *284*, 14628–14636.

Liu, M., Zhang, Y., Inouye, M., and Woychik, N.A. (2008). Bacterial addiction module toxin Doc inhibits translation elongation through its association with the 30S ribosomal subunit. Proc. Natl. Acad. Sci. USA *105*, 5885–5890.

Loris, R., Dao-Thi, M.H., Bahassi, E.M., Van Melderen, L., Poortmans, F., Liddington, R., Couturier, M., and Wyns, L. (1999). Crystal structure of CcdB, a topoisomerase poison from *E. coli*. J. Mol. Biol. *285*, 1667–1677.

Loris, R., Marianovsky, I., Lah, J., Laeremans, T., Engelberg-Kulka, H., Glaser, G., Muyldermans, S., and Wyns, L. (2003). Crystal structure of the intrinsically flexible addiction antidote MazE. J. Biol. Chem. *278*, 28252–28257.

Magnuson, R., and Yarmolinsky, M.B. (1998). Corepression of the P1 addiction operon by Phd and Doc. J. Bacteriol. *180*, 6342–6351.

Makarova, K.S., Wolf, Y.I., and Koonin, E.V. (2009). Comprehensive comparative-genomic analysis of type 2 toxin-antitoxin systems and related mobile stress response systems in prokaryotes. Biol. Direct *4*, 19.

Mattison, K., Wilbur, J.S., So, M., and Brennan, R.G. (2006). Structure of FitAB from *Neisseria gonorrhoeae* bound to DNA reveals a tetramer of toxin-antitoxin heterodimers containing pin domains and ribbon-helix-helix motifs. J. Biol. Chem. *281*, 37942–37951.

McKinley, J.E., and Magnuson, R.D. (2005). Characterization of the Phd repressor-antitoxin boundary. J. Bacteriol. *187*, 765–770.

Miallau, L., Faller, M., Chiang, J., Arbing, M., Guo, F., Cascio, D., and Eisenberg, D. (2009). Structure and proposed activity of a member of the VapBC family of toxin-antitoxin systems. VapBC-5 from *Mycobacterium tuberculosis*. J. Biol. Chem. *284*, 276–283.

Miki, T., Park, J.A., Nagao, K., Murayama, N., and Horiuchi, T. (1992). Control of segregation of chromosomal DNA by sex factor F in *Escherichia coli*. Mutants of DNA gyrase subunit A suppress letD (ccdB) product growth inhibition. J. Mol. Biol. *225*, 39–52.

Murshudov, G.N., Vagin, A.A., and Dodson, E.J. (1997). Refinement of macromolecular structures by the maximum-likelihood method. Acta Crystallogr. D Biol. Crystallogr. *53*, 240–255.

Murzin, A.G., Brenner, S.E., Hubbard, T., and Chothia, C. (1995). SCOP: a structural classification of proteins database for the investigation of sequences and structures. J. Mol. Biol. *247*, 536–540.

Nariya, H., and Inouye, M. (2008). MazF, an mRNA interferase, mediates programmed cell death during multicellular *Myxococcus* development. Cell *132*, 55–66.

Nicholls, A., Sharp, K.A., and Honig, B. (1991). Protein folding and association: insights from the interfacial and thermodynamic properties of hydrocarbons. Proteins *11*, 281–296.

Otwinowski, Z., and Minor, W. (1997). Processing of X-ray diffraction data collected in oscillation mode. Methods Enzymol. *276*, 307–326.

Pandey, D.P., and Gerdes, K. (2005). Toxin-antitoxin loci are highly abundant in free-living but lost from host-associated prokaryotes. Nucleic Acids Res. *33*, 966–976.

Pedersen, K., Christensen, S.K., and Gerdes, K. (2002). Rapid induction and reversal of a bacteriostatic condition by controlled expression of toxins and antitoxins. Mol. Microbiol. *45*, 501–510.

Pedersen, K., Zavialov, A.V., Pavlov, M.Y., Elf, J., Gerdes, K., and Ehrenberg, M. (2003). The bacterial toxin RelE displays codon-specific cleavage of mRNAs in the ribosomal A site. Cell *112*, 131–140.

Rost, B., Yachdav, G., and Liu, J. (2004). The PredictProtein server. Nucleic Acids Res. *32*, W321–W326.

Smith, J.A., and Magnuson, R.D. (2004). Modular organization of the Phd repressor/antitoxin protein. J. Bacteriol. *186*, 2692–2698.

Takagi, H., Kakuta, Y., Okada, T., Yao, M., Tanaka, I., and Kimura, M. (2005). Crystal structure of archaeal toxin-antitoxin RelE-RelB complex with implications for toxin activity and antitoxin effects. Nat. Struct. Mol. Biol. *12*, 327–331.

Terwilliger, T.C., and Berendzen, J. (1999). Automated MAD and MIR structure solution. Acta Crystallogr. D Biol. Crystallogr. *55*, 849–861.

Yamaguchi, Y., and Inouye, M. (2009). mRNA interferases, sequence-specific endoribonucleases from the toxin-antitoxin systems. Prog. Mol. Biol. Transl. Sci. *85*, 467–500.

Yarbrough, M.L., Li, Y., Kinch, L.N., Grishin, N.V., Ball, H.L., and Orth, K. (2009). AMPylation of Rho GTPases by *Vibrio* VopS disrupts effector binding and downstream signaling. Science *323*, 269–272.

Zhang, Y., and Inouye, M. (2009). The inhibitory mechanism of protein synthesis by YoeB, an *Escherichia coli* toxin. J. Biol. Chem. *284*, 6627–6638.

Zhang, Y., Zhang, J., Hoeflich, K.P., Ikura, M., Qing, G., and Inouye, M. (2003). MazF cleaves cellular mRNAs specifically at ACA to block protein synthesis in *Escherichia coli*. Mol. Cell *12*, 913–923.

Zhang, J., Zhang, Y., Zhu, L., Suzuki, M., and Inouye, M. (2004). Interference of mRNA function by sequence-specific endoribonuclease PemK. J. Biol. Chem. *279*, 20678–20684.

Zhang, Y., Yamaguchi, Y., and Inouye, M. (2009). Characterization of YafO, an *Escherichia coli* toxin. J. Biol. Chem. *284*, 25522–25531.

Note Added in Proof

A crystal structure has just been reported of a Phd-Doc complex containing a 4:1 ratio of Phd-to-Doc (Garcia-Pino et al. (2010). Cell *142*, 101-111), consistent with the heterogeneity in oligomeric state observed in the hydrodynamic studies reported in this paper.

